Design of frequency-domain beamforming solution for passive sonar systems in shallow-water environments

Nguyen Thi Nga*, Tran Quang Giang, Pham Van Hoa, Dang Viet Hung

Institute of Defense Equipment, Academy of Military Science and Technology, Hanoi, Vietnam.
*Corresponding author: ngadtvt@gmail.com
Received 7 Oct. 2025; Revised 5 Dec. 2025; Accepted 10 Dec. 2025; Published 25 Dec. 2025.
DOI: https://doi.org/10.54939/1859-1043.j.mst.108.2025.31-39

ABSTRACT

This paper develops the frequency-domain beamforming solution for passive sonar systems operating in shallow-water environments, where acoustic signals are significantly affected by multipath propagation and spatially varying attenuation. The study focuses on optimizing the beamforming configuration by analyzing the influence of key processing parameters, namely FFT length, window type, and overlap ratio, on system performance, including half-power beamwidth (HPBW), peak-to-sidelobe ratio (PSLR), and output signal-to-noise ratio (SNR_{out}). Simulation experiments were conducted using three narrowband sources at 800, 900, and 1200 Hz, representing the typical operational frequency range of passive sonar systems in shallow-water conditions. Based on the obtained results, the optimal Short-Time Fourier Transform (STFT) configuration is proposed to balance performance and computational cost within the 800–1200 Hz frequency band, offering practical applicability for passive sonar systems operating in the shallow water environment of Vietnam.

Keywords: Frequency-Domain Beamforming; Passive Sonar; STFT; SNR.

1. INTRODUCTION

Beamforming represents an essential technique in passive sonar systems for increasing the capability of detecting and accurately determining the direction of underwater targets [1, 2]. By employing a hydrophone array, beamforming performs spatial filtering to enhance signals arriving from the desired direction while reducing interference and noise from other directions [3]. Through coherent summing across array elements, beamforming significantly raises the signal-to-noise ratio (SNR) of the received signals [4], making it possible to identify weak targets in noisy environments and improving bearing estimation accuracy.

In broadband passive sonar, beamforming in the frequency domain offers various advantages. First, implementing the Fast Fourier Transform (FFT) to the signal received at each array element enables more computationally efficient processing of wideband signals [5]. By efficiently decomposing the broadband signal into narrowband components, or subbands, this approach enables the system to apply frequency-dependent weighting to each subband. Therefore, sources with various spectral characteristics can be separated more effectively, and processing can be adjusted jointly in both time and frequency domains [6]. In other words, frequency-domain beamforming allows selective processing across frequency, which is advantageous when multiple sources operate simultaneously in different frequency ranges.

Additionally, frequency-domain beamforming can be easily combined with spectral analysis techniques, such as time–frequency representations of acoustic signals. Short-Time Fourier Transform (STFT) spectra are commonly used for signal detection and classification [7]. The integration of beamforming with spectrogram-based analysis (e.g., generating angle–frequency plots) allows for visualizing and separating sources in both time and frequency dimensions. Recent studies have shown that exploiting the time–frequency distribution of signals enhances source direction estimation accuracy compared to full-band statistical methods; using individual time–frequency signatures enables more precise localization of acoustic sources [8]. Consequently,

frequency-domain beamforming offers improved capability in distinguishing closely spaced sources with different spectral characteristics.

Beyond classical techniques, recent studies have investigated flexible and reconfigurable array beamforming for underwater applications. Phan et al. [9] introduced a 2D hydrophone array configuration using adaptive sensor activation to form geometric subarrays and steer the mainlobe, showing that tailored array geometry and optimized weights can effectively control mainlobe width and sidelobe levels. A related study by Phan et al. [10] proposed a beam-shaping method for a cylindrical 3D hydrophone array, demonstrating improved directivity and sidelobe suppression through adaptive subarray selection. These studies highlight the critical role of array configuration in practical sonar design and complement the present work, which focuses on optimizing frequency-domain beamforming parameters.

However, the performance of frequency-domain beamforming depends on the parameters of STFT. Parameters such as the window type, FFT length, and frame overlap ratio have a significant impact on the system's resolution and accuracy. An inappropriate analysis window may cause spectral leakage, thereby degrading spatial filtering capability; an FFT length that is too short may lead to insufficient frequency resolution, while an excessively long one can introduce latency and time-varying noise effects. Similarly, the degree of frame overlap influences the temporal smoothness of the spectrogram. Therefore, it is essential to quantitatively evaluate the influence of these STFT parameters on beamforming performance in order to determine the optimal configuration for a passive sonar system operating in shallow-water environments.

The main contributions of this paper are summarized as follows:

• The frequency-domain beamforming system model is developed to analyze the spatial response of a passive sonar array.

• Comprehensive performance evaluation criteria, including Half-Power Beamwidth (HPBW), Peak-to-Sidelobe Ratio (PSLR), and output Signal-to-Noise Ratio (SNR_{out}), are employed to quantitatively assess the influence of STFT parameters on beamforming performance.

• An optimal configuration of STFT parameters is proposed for the 800–1200 Hz frequency band, aiming to enhance detection capability and directional resolution in passive sonar systems operating in shallow-water environments typical of the Vietnamese sea region.

The remainder of the paper is organized as follows. Section 2 describes the system design and solution development. Section 3 discusses the STFT parameters and evaluation criteria. Section 4 presents and analyzes the simulation results. Finally, Section 5 concludes the paper.

2. SYSTEM DESIGN AND SOLUTION DEVELOPMENT

2.1. Design system model

Consider a passive sonar system equipped with the hydrophone array of L elements shown in figure 1 [11]. The array can take various geometries, such as cylindrical, conical, or planar, depending on the application. The array elements are fixed in position, and their spacing may be uniform or non-uniform according to the design. When multiple underwater acoustic sources emit signals (e.g., submarine machinery noise, propeller noise, etc.), the acoustic waves arrive at the array elements with different time delays that depend on the direction of arrival (DOA) of each source. The acoustic propagation environment contains background noise originating from the ocean and onboard systems, typically modeled as broadband Gaussian noise, possibly including colored noise components with frequency correlation.

The signal received at the *i*-th array element [4] can be expressed as:

$$x_i(t) = \sum_{m=1}^{M} s_m(t - \tau_{i,m}) + n_i(t), \quad (1)$$

where M acoustic sources, $s_m(t)$ denotes the signal emitted by the m-th source, $\tau_{i,m}$ represents the time delay corresponding to the propagation from source m to the i-th hydrophone (depending on the direction of arrival θ_m and the distance), and $n_i(t)$ is the noise component at the i-th element. The objective of the beamforming processor is to combine the received signals $x_i(t)$ in such a way that the signal arriving from the desired direction θ is reinforced, while signals from other directions are suppressed.

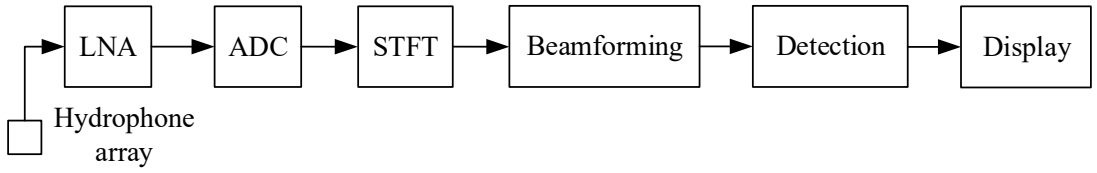

Figure 1. *Block diagram of the passive sonar system.*

The processing procedure is carried out through the following main steps:

****Short-time fourier transform (STFT)***

The analog signal $x_i(t)$ received at the i-th array element is first converted into a digital form through an analog-to-digital conversion (ADC). It is then analyzed in the frequency domain using the STFT [4], which is expressed as follows:

$$X_i(k,n) = \sum_{\tau=0}^{N-1} x_i(nH+\tau) w(\tau) e^{-j2\pi k\tau/N}, \tag{2}$$

where n denotes the time-frame index, k is the frequency-bin index, $w(\tau)$ represents the window function (e.g., Hamming, Hann, etc.), N is the window length (equivalently, the FFT length), and H is the hop size. The overlap between two consecutive frames is given by:

$$O = 1 - \frac{H}{N} \tag{3}$$

and can be expressed in percentage form as:

$$O(\%) = \frac{N-H}{N} \times 100\% \tag{4}$$

****Frequency-domain beamforming***

The digital signal $X_i(k,n)$ is beamformed in the frequency domain using the conventional Delay-and-Sum (DAS) method toward the steering direction θ [4, 11]:

$$Y(k,n,\theta) = \sum_{i=1}^{N} v_i(f_k,\theta) X_i(k,n), \tag{5}$$

where v_i denotes the steering vector corresponding to direction θ, and f_k is the frequency of the k-th bin.

$$v_i(f_k,\theta) = e^{-j2\pi f_k \tau_i(\theta)}. \tag{6}$$

****Beam scanning and spectral representation***

By varying the steering angle θ, the system can scan the beam across the entire surveillance sector (e.g., 0 - 360° in azimuth). For each θ at time frame n, the spectrum $|Y(k,n,\theta)|^2$ represents the energy distribution over frequency for that direction. To detect potential targets, the energy within specific frequency bands can be examined, either by integrating the spectrum over a selected frequency range or by identifying characteristic spectral peaks associated with the target.

This procedure illustrates the principle of frequency-domain beamforming: instead of applying time delays in the time domain, phase shifts are introduced in the frequency domain before summing the signals. This approach achieves the same beam-steering effect as narrowband beamforming but leverages the computational efficiency of the FFT, allowing effective processing of broadband signals and greater flexibility in frequency-domain analysis [7].

2.2. The analyzed STFT parameters

To evaluate the influence on beamforming performance, this study considers three primary parameters of the STFT: FFT length, window function, and frame overlap ratio.

***FFT length**

The FFT length N [4] determines the frequency resolution Δf with respect to the sampling frequency f_s as: $\Delta f = f_s / N$.

In beamforming applications, the longer FFT provides finer frequency resolution, allowing clearer separation of sources in the frequency domain; however, it reduces temporal sensitivity. Conversely, the shorter FFT captures rapid temporal variations but provides poorer frequency resolution, causing spectral overlap among sources. Therefore, N should be chosen to balance frequency and time resolution effectively.

***Window function**

The window function is employed to reduce spectral leakage outside the analysis band compared to the rectangular window. Common cosine-based windows include Hann, Hamming, and Blackman windows [12]. These windows attenuate the signal amplitude at the frame edges, thereby significantly suppressing the sidelobes of the resulting spectrum. However, this comes at the cost of an increased mainlobe width, which leads to reduced frequency resolution.

- The Hann and Hamming windows are often chosen as a compromise between leakage suppression and frequency resolution.

- The Blackman window provides very low leakage but may not be suitable when high frequency resolution is required.

***Frame overlap**

Frame overlap is applied to enhance the temporal smoothness of the spectrogram and to prevent data loss at frame boundaries [7]. An overlap ratio of 50% is commonly adopted for energy preservation, while 75% overlap produces a smoother spectrum at the expense of redundant information and increased computational cost.

In summary, by examining various configurations of FFT length, window function, and frame overlap, this study investigates their effects on beamforming performance, such as whether angular resolution is degraded by reduced frequency resolution, whether output SNR improves with an appropriate window function, and how the beam pattern is influenced by sidelobe behavior under different parameter settings.

2.3. Beamforming performance evaluation criteria

The performance of beamforming in passive sonar systems is evaluated based on several key criteria as follows:

***Angular resolution**

Angular resolution refers to the ability to distinguish between two acoustic sources with closely spaced directions of arrival. It is a crucial indicator of beam sharpness. The commonly used parameter is the HPBW of the main lobe, defined as the angular separation between the two points where the beam power drops by 3 dB from its peak [12]. A narrower main lobe (i.e., smaller HPBW) indicates higher angular resolution, meaning that two sources separated by only a small angle can still be resolved as distinct peaks in the beam pattern.

Output signal-to-noise ratio (SNR_{out})

The output SNR represents the signal-to-noise ratio of the beamformed signal in the target direction [4]. It is calculated by comparing the signal power of the desired source with the residual noise power at the beamformer signal. This metric reflects the array gain obtained by the beamforming process.

Half-power beamwidth (HPBW)

HPBW is defined as the angular width of the main beam measured at the −3 dB level relative to the peak [13]. This metric quantifies the spatial concentration of the beam, an effective beamformer should produce a sufficiently narrow main lobe to ensure accurate direction estimation. However, an excessively narrow beam may limit the spatial coverage and risk missing targets if phase distortions or environmental fluctuations occur.

Peak-to-sidelobe ratio (PSLR)

The sidelobe level represents the intensity of the highest sidelobe observed in the beam pattern after beamforming. Sidelobes characterize imperfect noise suppression or residual interference from undesired directions [13]. The PSLR is defined as the ratio between the main lobe peak and the maximum sidelobe peak, indicating the degree of spatial interference rejection.

By combining these criteria, HPBW, SNR_{out}, and PSLR, the overall beamforming performance can be comprehensively assessed in terms of angular resolution, signal enhancement capability, and background noise suppression. An effective system should exhibit a narrow main lobe, low sidelobe levels, and the significant SNR improvement. Nevertheless, these parameters involve inherent trade-offs: reducing sidelobes often broadens the main beam, while improving beam sharpness may lead to higher sidelobe levels [13]. Therefore, the objective is to determine an optimal configuration that balances these performance factors.

3. RESULTS AND DISCUSSION

3.1. Simulation configuration

The passive sonar system consists of a uniform linear array (ULA) with L = 136 hydrophone elements, spaced at half the wavelength. The narrowband source signal comprises three sinusoidal components with frequencies of 800 Hz, 900 Hz, and 1200 Hz. The sampling frequency is f_s = 20 kHz, and the direction of arrival (DOA) of the source signal is fixed at θ = 10°. The search domain for beamforming is scanned from −60° to +60°. The received signals were modeled with an input SNR level of 5 dB to evaluate the system performance under noise conditions.

The STFT analysis is conducted using multiple configurations: FFT lengths $N \in \{256, 512, 1024, 2048\}$, window functions (Hann, Hamming, and Blackman), and frame overlap ratios ranging from 25% to 75%.

To accurately model sound propagation, a geometric underwater acoustic channel model integrated with relevant environmental parameters [14] was employed. This model accounts for variations in water depth, surface and seabed boundaries, as well as the transmitter-receiver geometry, thereby capturing multipath propagation and reflection effects inherent in shallow waters.

Specifically, for the Vietnamese shallow-water scenario, the water depth was configured as 100 m, and the horizontal distance between the transmitter and receiver was 1000 m, with both positioned at a depth of 50 m. The sound speed was assumed to be 1500 m/s, with salinity of 35 ppt and temperature of 30 °C. The number of rays reflected from the sea surface and the seabed were set to 80 and 70, respectively, to capture the complex multipath structure characteristic of shallow-water acoustic channels.

3.2. Simulation results and discussion

Evaluation of FFT length (N)

A comparative analysis was conducted for different FFT lengths $N = 256$, 512, 1024 and 2048, using the same Hann window, 50% overlap, and a source frequency of $f = 800$ Hz with an input SNR of $SNR_{in} = 5$ dB. Table 1 and figure 2 illustrate the impact of FFT length on the performance of the passive sonar beamforming system.

The results presented in table 1 and figure 2 show that variations in FFT length (N) have only a minor effect on beam pattern geometry, as reflected in the nearly constant HPBW and PSLR values. Specifically, HPBW remains around 7.4°–7.8°, and PSLR stabilizes near 1.5–1.6 dB, indicating that increasing N does not significantly change the spatial selectivity of the beamformer. The output SNR shows a slight upward trend with increasing FFT length, improving from 9.25 dB at $N = 256$ to 9.35 dB at $N = 2048$, as presented in figure 2(a). This improvement corresponds to the ΔSNR curve, which also rises slightly, from 4.25 dB to 4.35 dB, as shown in figure 2(b).

Table 1. *Effect of FFT length on passive sonar system performance.*

No.	FFT Length (N)	HPBW (°)	PSLR (dB)	SNR_{out} (dB)
1	256	7,8	1,62	9,25
2	512	7,6	1,52	9,30
3	1024	7,4	1,52	9,34
4	2048	7,4	1,52	9,35

These results suggest that larger FFT lengths enhance frequency resolution, leading to marginal improvements in beamforming gain and noise suppression. Nevertheless, the performance gain saturates beyond $N = 1024$, implying that $N = 1024$ provides an effective trade-off between computational cost and performance.

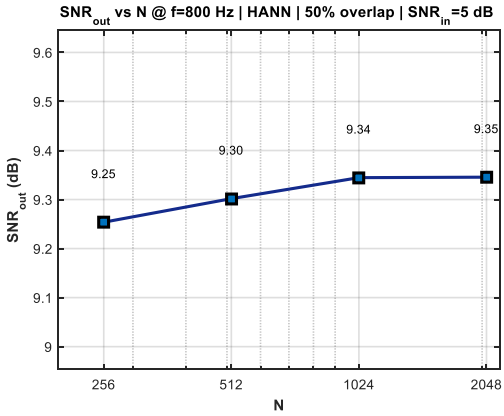

(a) SNR_{out} versus FFT length N.

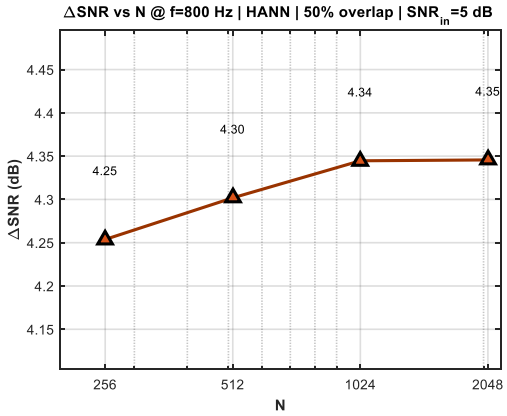

(b) ΔSNR versus FFT length N.

Figure 2. *Relationship between parameters in the passive sonar system.*

****Evaluation of frame overlap (O)***

The experiments were performed using overlap ratios of 0%, 25%, 50%, and 75%, with an FFT length of 1024, a Hann window, and source frequencies at 800, 900, and 1200 Hz, while maintaining a constant input SNR of 5 dB.

Table 2 presents the influence of the overlap parameter on the performance of the passive sonar beamforming system. These results indicate that variations in the frame overlap ratio have only a minor influence on the overall beamforming performance across all tested frequencies (800, 900, and 1200 Hz). The HPBW remains nearly constant for each frequency, approximately 7.4° at 800 Hz, 7.7° at 900 Hz, and 8.2° at 1200 Hz, confirming that the main-lobe width primarily depends on signal frequency and array geometry, rather than the overlap. The PSLR values are stable within a narrow range (≈ 1.5 – 1.6 dB) for all frequencies, demonstrating that the overlap parameter has negligible impact on sidelobe suppression, which is mainly determined by the window function.

The output SNR shows slight improvement as the overlap increases up to 50%, beyond which the enhancement becomes marginal. For instance, at 900 Hz, SNR_{out} increases from 9.306 dB (0%) to 9.312 dB (50%), indicating that moderate overlap improves spectral averaging and temporal smoothness of the STFT, thus stabilizing the beamforming output. However, further increasing the overlap to 75% yields almost no additional benefit while increasing computational cost. Therefore, the 50% overlap ratio provides the optimal balance between performance stability and computational efficiency for frequency-domain beamforming in passive sonar applications.

Table 2. *Effect of frame overlap on passive sonar system performance.*

Frequency (Hz)	Overlap (O, %)	HPBW (°)	PSLR (dB)	SNR_{out} (dB)
800	0	7,4	1,519	9,335
800	25	7,4	1,522	9,337
800	50	7,4	1,524	9,344
800	75	7,4	1,524	9,344
900	0	7,7	1,615	9,306
900	25	7,7	1,614	9,307
900	50	7,7	1,614	9,312
900	75	7,7	1,614	9,321
1200	0	8,2	1,485	9,207
1200	25	8,2	1,482	9,203
1200	50	8,2	1,480	9,201
1200	75	8,2	1,480	9,200

****Evaluation of window functions***

A comparison was carried out among the Hann, Hamming, and Blackman windows using FFT length $N = 1024$, 50% overlap, source frequency $f = 800$ Hz, and input SNR $SNR_{in} = 5$ dB. Table 3 summarizes the influence of the analysis window on passive sonar beamforming performance.

Table 3. *Effect of window function on passive sonar system performance.*

No.	Window Function	HPBW (°)	PSLR (dB)	SNR_{out} (dB)
1	Hann	7,4	1,522	9,344
2	Hamming	7,4	1,522	9,344
3	Blackman	7,4	1,524	9,345

The results depicted in table 3 show that the choice of window function (Hann, Hamming, or Blackman) has a negligible effect on the main-lobe width and overall beamforming performance under the given configuration ($N = 1024$, 50% overlap, $f = 800$, $SNR_{in} = 5$ dB). The HPBW remains constant at approximately 7.4° for all three window types, confirming that the main-lobe geometry is governed primarily by the array structure and operating frequency rather than the spectral window. The PSLR has a slight improvement observed with the Blackman window (1.524 dB) compared to Hann and Hamming (≈ 1.522 dB), which aligns with its stronger sidelobe attenuation properties. The output SNR values are nearly identical (~ 9.34 – 9.35 dB), indicating that the choice of window function has only a marginal influence on the beamforming gain under these test conditions.

In summary, the Blackman window provides a minor advantage in sidelobe suppression and marginally higher SNR, while Hann and Hamming windows offer nearly equivalent performance with lower computational overhead. Thus, the selection of the window function can be based on the desired trade-off between sidelobe reduction and implementation simplicity.

3.3. Computational complexity

The computational complexity of the frequency-domain beamforming system is dominated by two main processing stages: the Short-Time Fourier Transform (STFT) and the delay-and-sum

(DAS) beamforming operation. For an array with L hydrophones, an FFT size of N, and K time frames, the system operates efficiently due to the linear structure of DAS and the FFT computations.

The STFT stage constitutes the dominant computational cost of the system. Since each hydrophone performs one FFT per time frame, the overall STFT complexity is $O(LKN\log N)$, scaling linearly with the number of hydrophones and time frames and quasi-linearly with the FFT length. In comparison, the DAS beamformer requires only a weighted linear combination of the L hydrophones per frequency bin, resulting in a total cost of $O(LKN)$, which is substantially lower because it does not include the *logN* factor. Consequently, the computational burden is dominated by the FFT operations, while the DAS step adds only a lightweight linear overhead, making it suitable for real-time or large-array implementations. Increasing the FFT size or the overlap ratio directly increases the number of STFT computations, illustrating the trade-off between frequency resolution and computational efficiency.

4. CONCLUSIONS

The paper evaluates the frequency-domain beamforming performance of a passive sonar system designed for shallow-water environments representative of Vietnamese coastal regions, under various signal processing configurations. The experimental results indicate that the half-power beamwidth primarily depends on the signal frequency, whereas processing parameters such as FFT length, overlap ratio, and window type do not significantly alter the geometric characteristics of the main lobe. The FFT length N has a direct influence on frequency resolution and estimation quality, with $N = 1024$ providing an optimal balance between performance and computational cost. Increasing the overlap ratio to 50% improves both the stability and output SNR, while employing the Blackman window yields better sidelobe suppression and SNR enhancement compared with the Hann and Hamming windows.

REFERENCES

[1]. Wang Y et al., "*Null Broadening Beamforming for Passive Sonar Based on Weighted Similarity Vector*," Journal of Marine Science and Engineering, 11(10):1858, (2023).

[2]. B. Yin et al., "*Application of adaptive beamforming technology in underwater acoustic*," 2023 3rd International Conference on Neural Networks, Information and Communication Engineering (NNICE), Guangzhou, China, pp. 219-223, (2023).

[3]. J. Liu et al., "*Underwater three-hydrophone array passive ranging using time-dimensional Capon beamforming*," OCEANS 2019 - Marseille, Marseille, France, pp. 1-5, (2019).

[4]. L. J. Ziomek, "*An Introduction to Sonar Systems Engineering*," 2nd ed. New York: CRC Press, (2022).

[5]. J. A. Vásquez-Peralvo et al., "*Quantization Effects of Twiddle Factors in FFT for Beamforming Using Planar Arrays*," 2024 IEEE International Symposium on Phased Array Systems and Technology (ARRAY), Boston, MA, USA, pp. 1-7, (2024).

[6]. R. Palisetty et al., "*Area-Power Analysis of FFT Based Digital Beamforming for GEO, MEO, and LEO Scenarios*," 2022 IEEE 95th Vehicular Technology Conference: (VTC2022-Spring), Helsinki, Finland, pp. 1-5, (2022).

[7]. G. Itzhak et al., "*STFT-Domain Least-Distortion Region-of-Interest Beamforming*," in IEEE Transactions on Audio, Speech and Language Processing, vol. 33, pp. 2803-2816, (2025).

[8]. M. G. Amin et al., "*Direction Finding Based on Spatial Time-Frequency Distribution Matrices*," Digital Signal Processing,Vol. 10 (4), pp. 325-339, (2000).

[9]. P. H. Minh et al., "*The solution of configuration 2D hydrophone array based on beamforming option*," Journal of Military Science and Technology, vol. 54, pp. 95–105, (2018).

[10]. P. H. Minh et al., "*A solution to customize beamforming 3D cylinder hydrophone arrays based on 1H antennas in the MGK-400EM sonar system*," Journal of Military Science and Technology, Special Issue 9-2020, pp. 227–239, (2020).

[11]. H. L. Vantree, "*Optimum Array Processing: Part IV of Detection, Estimation, and Modulation Theory*," 1st ed. Wiley, (2002).

[12].J. G. Proakis et al., "*Digital Signal Processing*," 4th ed. Pearson, (2014).
[13].R. Mailloux, "*Phased Array Antenna Handbook*," 3rd ed. London: Artech House, (2017).
[14]. D. V. Ha et al., "*Methods of designing shallow underwater acoustic channel simulators*," Acoustics Australia, pp. 439–448, (2016).

TÓM TẮT

Thiết kế giải pháp beamforming miền tần số cho hệ thống sonar thụ động trong môi trường biển nông

Bài báo này phát triển giải pháp định hình chùm tia miền tần số cho các hệ thống sonar thụ động hoạt động trong môi trường nước nông, nơi tín hiệu âm bị ảnh hưởng đáng kể bởi sự lan truyền đa đường và suy giảm thay đổi theo không gian. Nghiên cứu tập trung vào việc tối ưu hóa cấu hình định hình chùm tia bằng cách phân tích ảnh hưởng của các thông số xử lý chính, cụ thể là độ dài FFT, loại cửa sổ và tỷ lệ chồng lấn, đến hiệu suất hệ thống, bao gồm độ rộng chùm tia bán công suất (HPBW), tỷ lệ đỉnh-thùy phụ (PSLR) và tỷ lệ tín hiệu trên nhiễu đầu ra (SNR_{out}). Các thí nghiệm mô phỏng đã được tiến hành bằng cách sử dụng ba nguồn băng hẹp ở tần số 800, 900 và 1200 Hz, đại diện cho dải tần số hoạt động điển hình của các hệ thống sonar thụ động trong điều kiện nước nông. Dựa trên các kết quả thu được, cấu hình Biến đổi Fourier thời gian ngắn (STFT) tối ưu được đề xuất để cân bằng hiệu suất và chi phí tính toán trong dải tần số 800 - 1200 Hz, mang lại khả năng ứng dụng thực tế cho các hệ thống sonar thụ động hoạt động trong môi trường nước nông của Việt Nam.

Từ khoá: Beamforming miền tần số; Sonar thụ động; STFT; SNR.